Suction feeding performance and prey escape response interact to determine feeding success in larval fish

Noam Sommerfeld[1,2] and Roi Holzman[1,2]

1 School of Zoology, Faculty of Life Sciences, Tel Aviv University, Tel Aviv 69978, Israel.

2 The Inter-University Institute for Marine Sciences, POB 469, Eilat 88103, Israel.

* Corresponding author: Roi Holzman <holzman@tauex.tau.ac.il>

Keywords: *Sparus aurata*, Reynolds numbers, feeding kinematics

Abstract

The survival of larval marine fishes during early development is strongly dependent on their ability to capture prey. Most larval fish capture prey by expanding their mouth cavity, generating a "suction flow" that draws the prey into their mouth. Larval fish dwell in a hydrodynamic regime of low Reynolds numbers, which has been shown to impede their ability to capture non-evasive prey. However, the marine environment is characterized by an abundance of evasive prey such as Copepods. These organisms can sense the hydrodynamic disturbance created by approaching predators and perform high-acceleration escape maneuvers. Using a 3D high-speed video system, we characterized the interaction between 8-33 day post hatching *Sparus aurata* larvae and prey from a natural zooplankton assemblage that contained evasive prey, and assessed the factors that determine the outcome of these interactions. Larvae showed strong selectivity for large prey that was moving prior to the initialization of the strike. As previously shown in studies with non-evasive prey, larval feeding success increased with increasing Reynolds numbers. However, larval feeding success was also strongly dependent on the prey's escape response. Feeding success was lower for larger, more evasive prey, indicating that larvae might be challenged in capturing their preferred prey. The kinematics of successful strikes resulted in shorter response time but higher hydrodynamic signature available for the prey. Thus, despite being "noisier", successful strikes on evasive prey depended on preceding the prey's escape response. Our results show that larval performance, rather than larval preferences, determines their diet during early development.

Introduction

The vast majority of marine fishes reproduce by external fertilization, producing small eggs (~1 mm) that drift into the open ocean (Houde 1987; Cowen and Sponaugle 2009; Barneche et al. 2018). Following a brief period of development (usually lasting several days, depending on the ambient temperature) larvae hatch from the egg and begin to feed autonomously (Hunter 1981; Houde 1987; Cowen and Sponaugle 2009). After metamorphosis, the larvae settle into their adult habitat, either pelagic or benthic. This strategy is termed the "bipartite life cycle", indicating that the planktonic larvae dwell in a habitat that differs from that of the adults (Hunter 1981; Houde 1987; Cowen and Sponaugle 2009). During the pelagic period, larval diets consist of micro- and macro-zooplankton. Similar to many adult fishes, larvae feed by closing the distance to their prey, then lunging towards it while opening their mouth and expanding their buccal cavity. The expansion of the mouth generates a flow of water that carries the prey into the mouth, potentially countering the escape response of the prey (Holzman et al. 2015; China et al. 2017).

During the first few weeks of their lives, larvae of marine fishes experience high mortality rates, eradicating >90% of individuals before they reach metamorphosis. Previous research has identified multiple agents for this mortality, including predation, advection to unsuitable habitats, low food concentrations, and diseases (Hjort 1914; Houde 1987, 2008). However, the hydrodynamic environment in which larvae dwell also impedes their feeding performance, leading to reduced feeding success, low feeding rates, and possibly starvation (China and Holzman 2014; Yavno and Holzman 2017; Koch et al. 2019). In general, the interaction between a solid (e.g. a prey) and the flow around it (e.g. the suction flow of a feeding fish) can be characterized by the dimensionless Reynolds number (Re), depicting the

ratio between inertial and viscous forces exerted on the solid particle (Vogel 1994). Larger objects in faster flows are characterized by a hydrodynamic environment of high Re, in which inertial forces dominate and flows can be turbulent. Smaller objects (such as zooplankton) in slower flows (such as the suction flows of larval fish) are characterized by a hydrodynamic environment of low Re, in which viscous forces dominate, and the flows can be laminar and reversible. Successful feeding events of *Sparus aurata* larvae on rotifers have been characterized by higher Re numbers compared to unsuccessful attempts (China and Holzman 2014; China et al. 2017). The increase in Re has been positively correlated with larval length, and mechanistically attributed to successful larvae expanding their buccal cavity faster (resulting in faster suction flows), and opening their mouth to a larger diameter (China and Holzman 2014; China et al. 2017). While much is known about the interaction between larval fish and inert prey (Hernández 2000; Krebs and Turingan 2003; China and Holzman 2014; China et al. 2017), this knowledge offers only a limited insight into the interaction in nature, in which potential prey species usually possess a high ability to sense and respond to approaching predators.

Copepods are often the dominant zooplankton within the pelagic habitat, and an important food source for both adult fish and their larvae. Marine pelagic copepods are highly sensitive to hydrodynamic disturbances, which they perceive via the movement of small sensory setae located on their antennae (Yen et al. 1992; Yen and Strickler 1996; Fields and Yen 1997). The setae bend under shear that may be generated by the movements of organisms (both predators and prey) near the copepod. Strong shear usually trigger an extremely fast escape response, in which a copepod can accelerate at ~300 ms^{-2} and speeds of ~ 0.5 ms^{-1} (Buskey and Hartline 2003; Strickler and Balázsi 2007). Both sensory and motor capacities of copepods improve over ontogeny, leading to a more efficient escape response.

In *Acarcia tonsa* and *Temora longicornis*, adult copepods were ~6 fold more sensitive than the nauplii (Fields and Yen 1997; Titelman 2001). Correspondingly, the capture probability of nauplii into an artificial siphon flow decreased sharply as they matured (Fields and Yen 1997).

It is well established that the ability to capture copepods confers an energetic advantage compared to feeding on other prey types, and that a copepod-based diet increase larval fish survival (Beaugrand et al. 2003; Olivotto et al. 2008; Piccinetti et al. 2014). Stomach content analysis of larval fishes generally reveal a preference for copepods over other prey types, and this preference increases with larval age (Pepin and Penney 1997; Sabatés and Saiz 2000; Fulford et al. 2006; Jackson and Lenz 2016). Such selectivity could result from an ontogenetic shift in larval preferences (i.e. larvae direct more attacks towards copepods as they mature), or from an ontogenetic improvement in larval preference (i.e. larvae experience higher success rates on copepods as they mature), or both. A computational model that calculated the suction forces exerted on escaping prey, predicted that larval ability to counter the prey's escape force improves dramatically with larval size and age (Yaniv et al. 2014). Accordingly, the diet of clownfish larvae (*Amphiprion ocellaris)* was shown to consist only of copepod nauplii (*Parvocalanus crassirostris*) in the first days post hatching (DPH), and these larvae transitioned to feed on adult copepods only at ~9 DPH (Jackson and Lenz 2016). However, the mechanism behind this pattern is still unclear. Additionally, while the vast majority of marine fishes reproduce by releasing small pelagic eggs and provide no parental care, clownfishes provide parental care for their demersal eggs and their larvae hatch at a relatively large size and developed state (Kavanagh and Alford 2003; Barneche et al. 2018). Therefore, it is unclear how the

107 performance of *Amphiprion* larvae compare with that of the poorly-developed smaller
108 larvae that hatch from pelagic eggs.

109 Our goal was to characterize the interaction between small pelagic larval fish and
110 prey from a natural zooplankton assemblage that contains evasive prey. Specifically, we
111 sought to (1) determine whether larvae are selective to evasive prey; (2) estimate the
112 variables that affect feeding success on such prey; and (3) characterize the effect of the
113 larvae's morphology and kinematics on the escape response of the prey. We used 8-33 DPH
114 *Sparus aurata* larvae, as these larvae hatch from small pelagic eggs, representing the
115 common strategy among marine fishes. Larvae and prey were filmed using two
116 synchronized high-speed cameras in a laboratory setup that provided 3D tracking of both
117 prey and predator.
118

119 **Methods**

120 *Study organisms*

121 We used gilthead sea-bream larvae (*Sparus aurata* Linnaeus, 1758) as our model for
122 larval feeding (Holzman et al. 2015). *S. aurata* is a pelagic spawner, hatching at ~3.5 mm.
123 Feeding initiates at ~5 DPH at a body length of ~4 mm. Larvae reach the stage of flexion at
124 ~21-24 DPH, at a length of 7-10 mm, depending on conditions. Larvae were provided by the
125 ARDAG commercial nursery (Eilat, Israel). Throughout the experiments larvae were kept at
126 19°C in aerated seawater at a salinity of 35 ppm. Larvae were obtained prior to daily
127 feeding, hence were food deprived for >12 hrs.

128 We used a natural assemblage of zooplankton as the prey in all experiments. Prey
129 were obtained by towing a zooplankton net from a boat cruising at low speed, or by a
130 swimmer, depending on the seasonal abundance of zooplankton in the coastal waters of the

131 Gulf of Aqaba, Eilat. Swimmers towed a 1m long, 100 µm zooplankton net with a mouth
132 diameter of ~0.5 m, while the boat towed a longer, 4 m long net. At the end of the tow, the
133 captured zooplankton was sieved through a 500 µm net to remove larger zooplankton,
134 including predatory arrow worms and other elongated organisms, and carefully transferred
135 into a 1 liter holding aerated container until the onset of experiments. A subsample was
136 observed under a stereoscopic microscope to verify that the sample was dominated by
137 copepods; if not, a new sample was obtained. Fresh zooplankton was collected daily for the
138 experiments.
139
140 *3D filming of prey acquisition strikes*
141 We tracked the 3D position of the larvae and their prey during prey acquisition
142 strikes using two synchronized high-speed cameras (Photron Fastcam SA6) operating at
143 1000 frames per second. Cameras were fitted with Navitar 6000 ultra-zoom lenses,
144 providing 1:3¼ magnification (i.e. a 1 mm long object is projected at 3.25 mm on the sensor)
145 with a depth of field of ~50 mm (Fig 1). Cameras were positioned such that their resolution
146 and magnification were identical. The field of view of each camera was ~ 40 mm x 30 mm
147 (W x H) at a resolution of 1920 x 1440 pixels. The cameras were positioned 45 cm apart, at
148 an angle of 35˚ relative to one another (Fig 1). The volume on which the two cameras were
149 focused was ~20 milliliters. To minimize reflections and distortions and maximize the depth
150 of field, the aquarium was constructed such that each phase was perpendicular to one
151 camera. Two rectangular 2.2 watt LED lights were positioned behind the aquarium,
152 providing a backlight illumination of the visualized volume. Reconstruction of points in the
153 3D space was done using the package DLTdv5 in MATLAB (Hedrick 2008). The system was
154 calibrated at the beginning of each recording session using a calibration grid of 60 points,

155 spanning the visualized volume. Accuracy was assessed by measuring four known distances
156 in three different images, and estimated as <1.5%.

157 For each filming session, 5-15 larvae were introduced into the filming chamber and
158 given several minutes to acclimate. A random assortment of prey was then introduced into
159 the chamber using a pipette, and the fish were allowed to feed freely for ~30 min. The
160 system was triggered manually upon the observer's detection of a predator's feeding
161 attempt or a prey's escape response in the visualized volume. Thus, our dataset included
162 clips that featured: (1) predatory strikes in which the prey initiated an escape response; (2)
163 predatory strikes in which the prey did not move; and (3) escape responses executed by the
164 prey before the predator opened their mouth. For each strike, the time of strike initiation
165 (t=0) was defined as the time at which the prey started to escape (cases 1 & 3 above) or as
166 the time when the larvae opened its mouth (case 2). Note that these times were highly
167 correlated (r=0.75) in case 1. Overall, these events involved ~100 larvae ranging in age from
168 8 to 33 DPH (3-20 mm; Fig 1).

169 For the two views of each recorded event (from the two cameras that comprise the
170 system) four landmarks were digitized in each frame: the anterior tip of the upper jaw, the
171 anterior tip of the lower jaw, a point on the body (center of the eye), and a point on the
172 prey denoting the edge closest to the fish's mouth. Four additional landmarks were digitized
173 in one of the frames: (1) a point on the prey denoting the edge furthest from the fish's
174 mouth, (2) the base of the larva's caudal fin (3 & 4) the two vertices on the horizontal major
175 axis of an imaginary ellipse encapsulating the prey. Digitized 2D coordinates of the
176 landmarks from the paired cameras were converted to an earthbound 3D coordinate system
177 using DLTdv5. We used the coordinates of the landmarks to calculate the following
178 variables: (1) larval length, calculated as the distance between the center of the mouth to

179 the base of the caudal fin; (2) mouth gape (mm; hereafter "gape"), calculated at each point
180 in time as the distance between the anterior tip of the upper and lower jaw; (3) time to
181 peak gape (TTPG; ms), calculated as the time it took the larva to open its mouth to 95% of
182 maximal gape diameter; (4) gape opening speed (mm/s), calculated as the derivative of
183 gape diameter with time; (5) response distance (mm), the distance of the prey from mouth
184 center at the time of strike initiation; (6) larval swimming speed (mm/s) calculated as the
185 average speed of the larva during the feeding attempt; (7) the time to prey capture (ms); (8)
186 prey cruising speed (mm/s), calculated based on the displacement of the prey 10 frames
187 before the predator's strike (of prey escape) was initiated; (9) prey escape speed (mm/s),
188 calculated based on the displacement of the prey during its escape, usually <10 frames; and
189 (10) prey length (mm). We used these values to calculate the Reynolds number (equation 1)
190 for feeding and swimming of the larvae. Re was calculated as

191 $$Re = \frac{\rho l U}{\mu} \qquad \text{(eq.1)}$$

192 where ρ is the density (1024 kg m^{-3}) and μ is the dynamic viscosity (Pa s^{-1}) of the fluid.
193 $Re_{(feeding)}$ was calculated using maximal gape diameter as the relevant length (*l*; m) and the
194 peak suction flow speed (*U*; ms^{-1}). The latter speed was estimated based on TTPG, maximal
195 gape, and estimated buccal dimensions (Yaniv et al. 2014; China et al. 2017). $Re_{(swimming)}$ was
196 calculated using the larva length as the relevant length (*l*; m), and the larval swimming
197 speed as the flow velocity (*U*; ms^{-1}).

198 *Determinants of feeding success*

199 We used logistic regression to test the effect of the kinematic and morphological
200 traits of both prey and predator on feeding success. The dependent variable was larval
201 feeding success (fail *vs* success; binary variable). The independent variables were selected
202 following China et al (China et al. 2017), who found that the variance in feeding success on

non-evasive prey was explained only by the hydrodynamic environment (Re). Because our prey was evasive, we also included variables that can affect the prey's performance, i.e. whether it initiated an escape response (yes/no; binary variable), prey length, response distance, and prey swimming speed (before the strike was initiated). We used a model averaging approach to identify and weight the variables that affect feeding success. We used the function dredge (Barto'n 2017) to identify the best supported models (with ΔAIC < 2 relative to the best model), followed by calculation of model averaged estimates of the effect size and standard error for each variable (Claeskens and Hjort 2008).

We used a logistic regression model to test which variables determined the prey's escape response. Copepods are known to execute an escape response when exposed to high strain rates. These can be caused by the body of the approaching predator, in which case the disturbance is expected to increase with the swimming speed of the predator, the radius of the fish's head, and the distance between the predator and prey. Kiørboe (Kiørboe 2008) estimated this disturbance (γ; s^{-1}) as

$$\gamma = \frac{3\left(2a^2Rv+aR^2v\right)}{2(a+R)^2}$$

where R is the distance between the anterior end of the larvae and the prey (m), a is the radius of the larva's head (m), and ν is the swimming speed of the larvae (ms^{-1}). Our model therefore included prey length, larval swimming speed, the radius of the larva's head, and strike initiation distance as independent variable, and prey escape as a binary dependent variable.

Selectivity

We characterized the prey available to the larvae before each strike by measuring the length and tracking the motion of all potential prey items located within the larvae's

226 reactive volume. That volume was defined as a hemisphere with a diameter of 1 larval body
227 length, centered at the larvae's mouth, and with the plane passing through the center of the
228 hemisphere perpendicular to the larva's long axis (Fig 2). We used only strikes in which the
229 reactive volume contained more than one prey (N=90). We tested the effect of the length
230 (mm) and motion (binary variable: moving/stationary) on the probability of a larvae striking
231 a prey item using conditional logistic regression. In this analysis, each strike was considered
232 a choice experiment, incorporated into the model as a stratum [i.e. random variable; (Aizaki
233 and Nishimura 2008)].
234
235 **Results**
236 *Selectivity*
237 In all strikes in which more than one prey was present at a distance of 1 larval
238 length, attacks were directed towards the larger, moving prey (conditional logistic
239 regression; P<0.001 for size and P<0.007 for movement; whole model R2 = 0.26, P<0.001;
240 N=90 strikes and 223 prey items; Fig 2; Table 1). The logistic regression indicated that a 1
241 mm increase in the size of the prey would double the probability of attack, and that prey
242 movement would increase attack probability by four-fold (Table 1). Accordingly, the size of
243 attacked prey ranged from 0.06 to 1.5 mm (median 0.36 mm) and that of ignored prey
244 ranged 0.06-0.9 mm (median 0.18). Roughly two-thirds of the attacks were directed at prey
245 that were moving before the strike was initiated (Fig 2).
246 *Strike success*
247 A model selection procedure identified seven models that best predict strike
248 outcome based on the independent variables (Table 2). The R^2 for the models ranged from
249 0.54 to 0.59. A model averaging procedure on the selected models revealed that prey

capture significantly increased when prey did not attempt an escape response, when prey length was smaller, and when $Re_{(feeding)}$ was higher (all $P<0.05$; Table 2; Fig 3). This procedure also provides the relative importance values of each term, calculated as a sum of the Akaike weights over all of the models in which the term appears. The absence of an escape response was the most important predictor of strike success (relative rank =1), followed by $Re_{(feeding)}$ (0.9), $Re_{(swimming)}$ (0.89), prey length (0.8), strike initiation distance (0.56), and prey swimming speed (0.43).

Prey escape response

Prey escape response was the most important factor that determined the feeding success (see above). We therefore used a logistic regression model to test which factors affect the probability of the prey producing such a response. The model indicated that increasing larval speed and decreasing strike initiation distance significantly reduced the probability of escape response by the prey ($P < 0.006$ for both, $R2 = 0.42$; Table 3; Fig 4), whereas the effect of the other variables was non-significant. Thus, the response time available for the prey (strike initiation distance divided by larval speed) was shorter for prey that did not escape (mean ± SE = 0.01 ± 0.0025 seconds) than for prey that did escape (0.07 ± 0.01 seconds; Fig 4B). Additionally, the mean hydrodynamic disturbance (γ, s^{-1}) was lower for prey that did escape than for prey that did not escape (mean ± SE = 12.3 ± 2.0 s^{-1} and 21.2 ± 2.4 s^{-1} for escaping and non-escaping prey, respectively; Fig 4C).

Discussion

In this study, we characterized the interaction between larval fish and prey present in a natural zooplankton assembly that was dominated by evasive prey. Larvae showed a strong selectivity for large prey that were moving prior to the initialization of the larva's

274 strike (Fig 2). As previously shown in studies with non-evasive prey, we found that larval
275 feeding success increased with increasing Reynolds numbers (Fig 3). However, larval
276 feeding success was also strongly dependent on the prey's escape response (Table 2).
277 Feeding success was lower for larger, more evasive prey (Fig 3), indicating that larvae might
278 be challenged in capturing their preferred prey. The kinematics of strikes on escaping prey
279 were characterized by slower larval swimming speed and greater strike initiation distance
280 compared to strikes on non-escaping prey (Fig 4; Table 3). These kinematics resulted in
281 shorter response time and higher hydrodynamic disturbance for prey that did not escape
282 (Fig 4).

283 Previous studies of feeding success by larval fish have focused on their interactions
284 with non-evasive prey (Hernández 2000; Krebs and Turingan 2003; China and Holzman
285 2014; China et al. 2017) although several studies have reported on interactions between
286 copepods and clownfish larvae (Jackson and Lenz 2016; Robinson et al. 2019; Tuttle et al.
287 2019). In small marine larvae that hatch from pelagic eggs, the hydrodynamic environment
288 (denoted by Re) is the dominant factor that determines larval kinematics and prey capture
289 performance. However, clownfish larvae hatch at a well-developed state following parental
290 care of the eggs, and likely live in a realm of higher Re. It is therefore unclear how their
291 interactions with evasive prey represent the general case across larvae of marine fish, and a
292 direct comparison of the predatory strategies of representative larvae from these two life-
293 history strategies is warranted.

294 In general, the dynamics of the predator-prey interactions can change due to the
295 prey's escape response. A CFD model of larval suction flows showed that smaller (younger)
296 larvae would be able to capture only weakly evasive prey that are attacked from a short
297 distance [relative to their mouth diameter (Yaniv et al. 2014)]. The predictions of that CFD

298 model for inert prey were the opposite: that the distance in which such prey could be
299 captured decreased through ontogeny (Yaniv et al. 2014). Observations on *Amphiprion*
300 *ocellaris* larvae feeding on the calanoid copepod *Bestiolina similis* (Jackson and Lenz 2016;
301 Tuttle et al. 2019) revealed that feeding success on evasive prey increased throughout
302 ontogeny, and that older larvae were able to capture more evasive prey and from a greater
303 distance compared to younger larvae. The results of the present study (Fig 4A) further
304 corroborate the CFD prediction (Yaniv et al. 2014), and demonstrate that for interactions
305 with evasive prey, Reynolds number is not the only parameter that determines strike
306 success (Table 2). Specifically, the ability of the prey to execute an escape response at the
307 right time is critically important in determining the outcome of this predator-prey
308 interaction (Table 2). In predator-prey interactions between adult zebrafish and their prey
309 (larval zebrafish), prey that did not initiated an escape response were always captured,
310 whereas escape responses that were timed correctly resulted in prey escape (Stewart et al.
311 2013). In the present study, prey that did not escape were not always captured, likely due to
312 the larva's inability to produce sufficiently strong suction flows. Thus, in larval fish, prey
313 capture is determined on the one hand by the ability of the larva to execute a high-Re strike;
314 and on the other hand by the ability of the prey to execute a timely escape response (Fig 3,
315 4).

316 Copepods are well-known for their ability to execute high-acceleration escape
317 responses when sensing a hydrodynamic disturbances (Yen et al. 1992; Fields and Yen 1997;
318 Buskey et al. 2002; Tuttle et al. 2019). Viitasalo et al (Viitasalo et al. 1998) assessed the
319 factors that determine the success of predatory strikes by adult three-spine sticklebacks on
320 two species of copepods. They concluded that feeding success was limited to cases in which
321 the fish was able to approach the copepod slowly. In those cases, the hydrodynamic signal

322 available to the copepod was weaker, resulting in a late escape response and a shorter
323 reaction distance to the approaching predator (Viitasalo et al. 1998). Similar results were
324 observed for *Amphiprion ocellaris* larvae feeding on the calanoid copepod *Bestiolina similis*
325 (Tuttle et al. 2019). In the present study we found an opposite trend: feeding success was
326 limited to cases in which the larvae swam quickly towards the prey. Similar to sticklebacks,
327 prey capture success was associated with short reaction distances. In *S. aurata* larvae, the
328 strike kinematics on prey that eventually executed an escape response resulted in a longer
329 response time and lower hydrodynamic disturbance (Fig 4). We suggest that this trend
330 might reflect the larvae's inability to correctly time their strike. Striking from too far would
331 allow evasive prey long enough time (~70 ms; Fig 4B) to respond to the hydrodynamic
332 disturbance produced by the predator. Conversely, a stealth approach followed by a fast
333 lounge might provide the prey with little time (<10 ms) to respond to the predator (Tuttle et
334 al. 2019). Thus, despite being "noisier", successful strikes on evasive prey might depend on
335 striking fast to precede the prey's escape response. Alternatively, it could also be that the
336 predators are able to distinguish weakly evasive prey and change their kinematics
337 accordingly.

338 In general, adult fishes show a strong selectivity for large prey (O'Brien et al. 1976;
339 Gardner 1981; Li et al. 1985; Holzman and Genin 2003, 2005). Werner and Hall (Werner and
340 Hall 1974) suggested that such size selection is related to the optimal allocation of time
341 spent searching and handling prey. In contrast, larval fish are considered selective for
342 smaller, less evasive prey, at least in the first days after exogeneous feeding initiates (Pepin
343 and Penney 1997; Sabatés and Saiz 2000; Fulford et al. 2006; Jackson and Lenz 2016). It is
344 nevertheless unclear why selectivity for small prey might be optimal for larvae. However,
345 studies on larval fish selectivity have largely been based on assessing the depletion of prey

346 within an experimental container, or on a comparison between the prey found within the
347 guts of larvae and that in the environment. Either way, such studies integrate two processes
348 within the predator-prey interaction: the first being the recognition and approach to the
349 prey; and the second being the strike itself. In the first stage, selectivity can develop
350 following a bias towards a preferred prey, or due to a difference in prey detectability, with
351 both resulting in a higher attempt rate on a certain prey type (Werner and Hall 1974; Li et al.
352 1985; Buskey et al. 1993; Holzman and Genin 2005). In the second stage, selectivity can
353 develop following a bias in the ability of the predator to capture certain prey types that that
354 better escape or defend themselves. Our experimental system provides novel insights into
355 the role of each stage in determining larval selectivity. Larvae show a strong preference for
356 directing predatory strikes towards larger, moving prey (Fig 2). However, this preference
357 would not be reflected in their diet, because such prey is more likely to successfully escape
358 (Fig 2, 3). Thus, the apparent selectivity for smaller prey by younger fish larvae could be the
359 result of a prey-size-dependent capture success rather than an active preference for smaller
360 prey.
361

362 References

363 Aizaki, H., and K. Nishimura. 2008. Design and Analysis of Choice Experiments Using R: A
364 Brief Introduction. Agricultural Information Research 17:86–94.

365 Barneche, D. R., S. C. Burgess, and D. J. Marshall. 2018. Global environmental drivers of
366 marine fish egg size. Global Ecology and Biogeography 27:890–898.

367 Barto'n, K. 2017. MuMIn: Multi-Model Inference. R package.

368 Beaugrand, G., K. M. Brander, J. Alistair Lindley, S. Souissi, and P. C. Reid. 2003. Plankton
369 effect on cod recruitment in the North Sea. Nature 426:661–664.

370 Buskey, E. J., C. Coulter, and S. Strom. 1993. Locomotory patterns of microzooplankton:
371 potential effects on food selectivity of larval fish. Bulletin of Marine Science 53:29–43.

372 Buskey, E. J., and D. K. Hartline. 2003. High-speed video analysis of the escpae response of
373 the copepod Acartia tonsa to shadows. Biol Bull 204:28–37.

374 Buskey, E. J., P. H. Lenz, and D. K. Hartline. 2002. Escape behavior of planktonic copepods in
375 response to hydrodinamic disturbances: high speed video analysis. Marine Ecology Progress
376 Series 235:135–146.

377 China, V., and R. Holzman. 2014. Hydrodynamic starvation in first-feeding larval fishes.
378 Proceedings of the National Academy of Sciences of the United States of America 111:8083–
379 8.

380 China, V., L. Levy, A. Liberzon, T. Elmaliach, and R. Holzman. 2017. Hydrodynamic regime
381 determines the feeding success of larval fish through the modulation of strike kinematics.
382 Proceedings of the Royal Society B: Biological Sciences 284.

383 Claeskens, G., and N. L. Hjort. 2008. Model selection and model averaging. Cambridge
384 University Press.

385 Cowen, R. K., and S. Sponaugle. 2009. Larval Dispersal and Marine Population Connectivity.

386 Annu. Rev. Mar. Sci 1:443–66.

387 Fields, D. M., and J. Yen. 1997. The escape behavior of marine copepods in response to a

388 quantifiable fluid mechanical disturbance. Journal of Plankton Research 19:1289–1304.

389 Fulford, R. S., J. A. Rice, B. Belonger, J. M. Dettmers, F. P. Binkowski, and T. J. Miller. 2006.

390 Foraging selectivity by larval yellow perch (*Perca flavescens*): implications for understanding

391 recruitment in small and large lakes. Canadian Journal of Fisheries and Aquatic Sciences

392 63:28–42.

393 Gardner, M. B. 1981. Mechanisms of Size Selectivity by Planktivorous Fish: A Test of

394 Hypotheses. Ecology 62:571–578.

395 Hedrick, T. L. 2008. Software techniques for two- and three-dimensional kinematic

396 measurements of biological and biomimetic systems. Bioinspiration & biomimetics

397 3:034001.

398 Hernández, L. P. 2000. Intraspecific scaling of feeding mechanics in an ontogenetic series of

399 zebrafish, Danio rerio. The Journal of experimental biology 203:3033–43.

400 Hjort, J. 1914. Fluctuations in the great fisheries of northern Europe. Rapp. Pa-V. Reun.

401 Cons. Perm. Int. Explor. Mer 19:1–228.

402 Holzman, R., V. China, S. Yaniv, and M. Zilka. 2015. Hydrodynamic Constraints of Suction

403 Feeding in Low Reynolds Numbers, and the Critical Period of Larval Fishes. Integrative and

404 Comparative Biology 55:48–61.

405 Holzman, R., and A. Genin. 2003. Zooplanktivory by a nocturnal coral-reef fish: Effects of

406 light, flow, and prey density. Limnology and Oceanography 48:1367–1375.

407 ———. 2005. Mechanisms of selectivity in a nocturnal fish: A lack of active prey choice.

408 Oecologia 146:329–336.

409 Houde, E. D. 1987. Fish Early Life Dynamics and Recruitment Variability. Page 2: 17-29 *in*

410 American Fisheries Society Symposium (Vol. 2).

411 Houde, E. D. 2008. Emerging from Hjort's shadow. Journal of Northwest Atlantic Fishery

412 Science 41:53–70.

413 Hunter, J. R. 1981. Feeding ecology and predation of marine fish larvae. Pages 33–79 *in* R.

414 Lasker, ed. Marine Fish Larvae. University of Washington Press, Seattle.

415 Jackson, J. M., and P. H. Lenz. 2016. Predator-prey interactions in the plankton: larval fish

416 feeding on evasive copepods. Scientific Reports 6:33585.

417 Kavanagh, K. D., and R. A. Alford. 2003. Sensory and skeletal development and growth in

418 relation to the duration of the embryonoic and larval stages in damselfishes

419 (Pomacentridae). Biological Journal of the Linnean Society 80:187–206.

420 Kiørboe, T. 2008. A mechanistic approach to plankton ecology. Princeton University Press.

421 Koch, L., I. Shainer, T. Gurevich, and R. Holzman. 2019. The Expression of *agrp1* , A

422 Hypothalamic Appetite-Stimulating Neuropeptide, Reveals Hydrodynamic-Induced

423 Starvation in a Larval Fish. Integrative Organismal Biology 1.

424 Krebs, J. M., and R. G. Turingan. 2003. Intraspecific variation in gape – prey size relationships

425 and feeding success during early ontogeny in red drum, *Sciaenops ocellatus*. Environmental

426 Biology of Fishes 66:75–84.

427 Li, K. T., J. K. Wetterer, and N. G. Hairston. 1985. Fish Size, Visula Resolution, and Prey

428 Selectivity. Ecology 66:1729–1735.

429 O'Brien, W. J., N. A. Slade, and G. L. Vinyard. 1976. Apparent Size as the Determinant of Prey

430 Selection by Bluegill Sunfish (*Lepomis Macrochirus*). Ecology 57:1304–1310.

431 Olivotto, I., I. Buttino, M. Borroni, C. C. Piccinetti, M. G. Malzone, and O. Carnevali. 2008.

432 The use of the Mediterranean calanoid copepod Centropages typicus in Yellowtail clownfish

433 (*Amphiprion clarkii*) larviculture. Aquaculture 284:211–216.

434 Pepin, P., and R. W. Penney. 1997. Patterns of prey size and taxonomic composition in larval
435 fish: are there general size-dependent models? Journal of Fish Biology 51:84–100.
436 Piccinetti, C. C., F. Tulli, N. E. Tokle, G. Cardinaletti, and I. Olivotto. 2014. The use of
437 preserved copepods in sea bream small-scale culture: biometric, biochemical and molecular
438 implications. Aquaculture Nutrition 20:90–100.
439 Robinson, H., J. Strickler, M. Henderson, D. Hartline, and P. Lenz. 2019. Predation strategies
440 of larval clownfish capturing evasive copepod prey. Marine Ecology Progress Series
441 614:125–146.
442 Sabatés, A., and E. Saiz. 2000. Intra- and interspecific variability in prey size and niche
443 breadth of myctophiform fish larvae. Marine Ecology Progress Series 201:261–271.
444 Stewart, W. J., G. S. Cardenas, and M. J. Mchenry. 2013. Zebrafish larvae evade predators by
445 sensing water flow. The Journal of Experimental Biology 216:388–398.
446 Strickler, J. R., and G. Balázsi. 2007. Planktonic copepods reacting selectively to
447 hydrodynamic disturbances. Philosophical transactions of the Royal Society of London.
448 Series B, Biological sciences 362:1947–1958.
449 Titelman, J. 2001. Swimming and escape behavior of copepod nauplii: Implications for
450 predator-prey interactions among copepods. Marine Ecology Progress Series 213:203–213.
451 Tuttle, L. J., H. E. Robinson, D. Takagi, J. R. Strickler, P. H. Lenz, and D. K. Hartline. 2019.
452 Going with the flow: hydrodynamic cues trigger directed escapes from a stalking predator.
453 Journal of The Royal Society Interface 16:20180776.
454 Viitasalo, M., T. Kiorboe, J. Flinkman, L. W. Pedersen, and A. W. Visser. 1998. Predation
455 vulnerability of planktonic copepods: Consequences of predator foraging strategies and prey
456 sensory abilities. Marine Ecology Progress Series 175:129–142.
457 Vogel, S. 1994. Life in moving fluids: the physical biology of flow. Second edition. Princeton

University Press.

Werner, E. E., and D. J. Hall. 1974. Optimal Foraging and the Size Selection of Prey by the Bluegill Sunfish (*Lepomis Macrochirus*). Ecology 55:1042–1052.

Yaniv, S., D. Elad, and R. Holzman. 2014. Suction feeding across fish life stages: flow dynamics from larvae to adults and implications for prey capture. The Journal of experimental biology 217:3748–57.

Yavno, S., and R. Holzman. 2017. Do viscous forces affect survival of marine fish larvae? Revisiting the 'safe harbour' hypothesis. Reviews in Fish Biology and Fisheries. 28: 201–212.

Yen, J., P. H. Lenz, D. V. Gassie, and D. K. Hartline. 1992. Mechanoperception in marine copepods: electrophysiological studies on the first antennae. Journal of Plankton Research 14:495–512.

Yen, J., and J. R. Strickler. 1996. Advertisement and concealment in the plankton: What makes a copepod hydrodynamically conspicuous. Invertebrate Biology 115:191–205.

473 Table 1: Conditional logistic regression model depicting the effect of prey's length
474 (mm) and motion (binary variable: moving/stationary) on the probability of a fish
475 attempting to capture it. SE- adjusted standard error of the estimate.

	Estimate	SE	Z value	P
Size	4.07	1.50	2.71	0.007
Motion	2.17	0.43	5.05	0.0001

476

477

478

479

480 Table 2: Conditional average from the seven best logistic regression models
481 depicting the effect of independent variable on feeding success. SE- adjusted standard error
482 of the estimate. Rank is the relative importance values of each term, calculated as a sum of
483 the Akaike weights over all of the models in which the term appears.

	Estimate	SE	Z value	P	Rank
Intercept	1.31	0.86	1.52	0.127	
Prey escape (Y/N)	-2.04	0.77	2.66	0.008	1
Prey length	-6.66	2.97	2.23	0.025	0.8
Re (feeding)	0.04	0.016	2.11	0.034	0.9
Re (swimming)	0.004	0.002	1.75	0.080	0.89
Strike initiation distance	-2.78	1.80	1.54	0.124	0.56
Prey speed	-0.095	0.080	1.18	0.238	0.43

484

485

Table 3: Logistic regression model depicting the effect of the independent variable on prey escape response. The model's R^2 was 0.42. SE- adjusted standard error of the estimate.

	Estimate	SE	Z value	P
Intercept	-0.43	0.90	-0.47	0.63
Prey length	2.50	1.73	1.44	0.14
Larval speed	-0.04	0.01	-4.46	<0.001
Head radius	0.32	2.78	0.11	0.91
Strike initiation distance	3.24	1.18	2.74	0.006

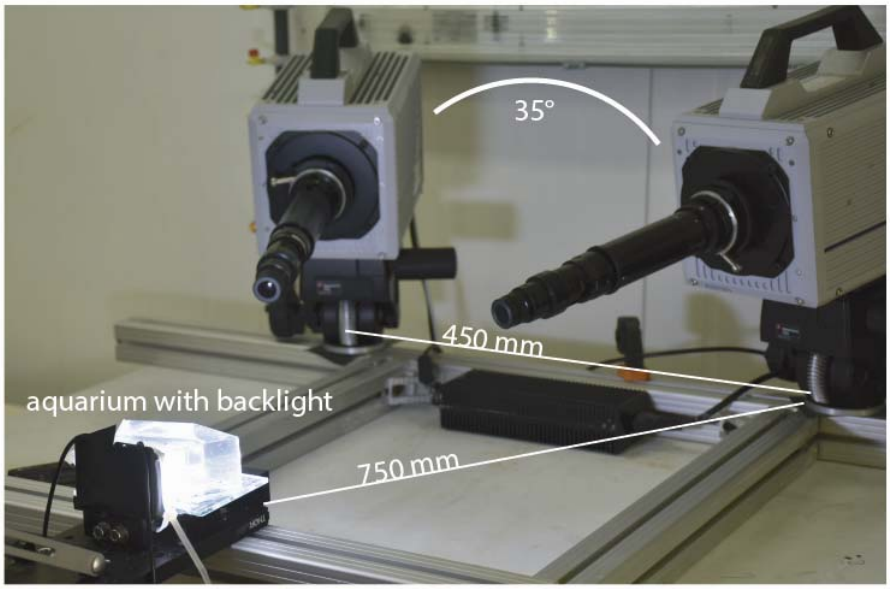

491

492 Fig 1: The positions of the larvae and their prey were tracked in 3D using two

493 synchronized high-speed cameras (Photron Fastcam SA6) fitted with Navitar 6000 ultra-

494 zoom lenses. The lenses provided 1:3¼ magnification with a depth of field of ~50 mm. Data

495 were collected at 1000 frames per second.

496

497

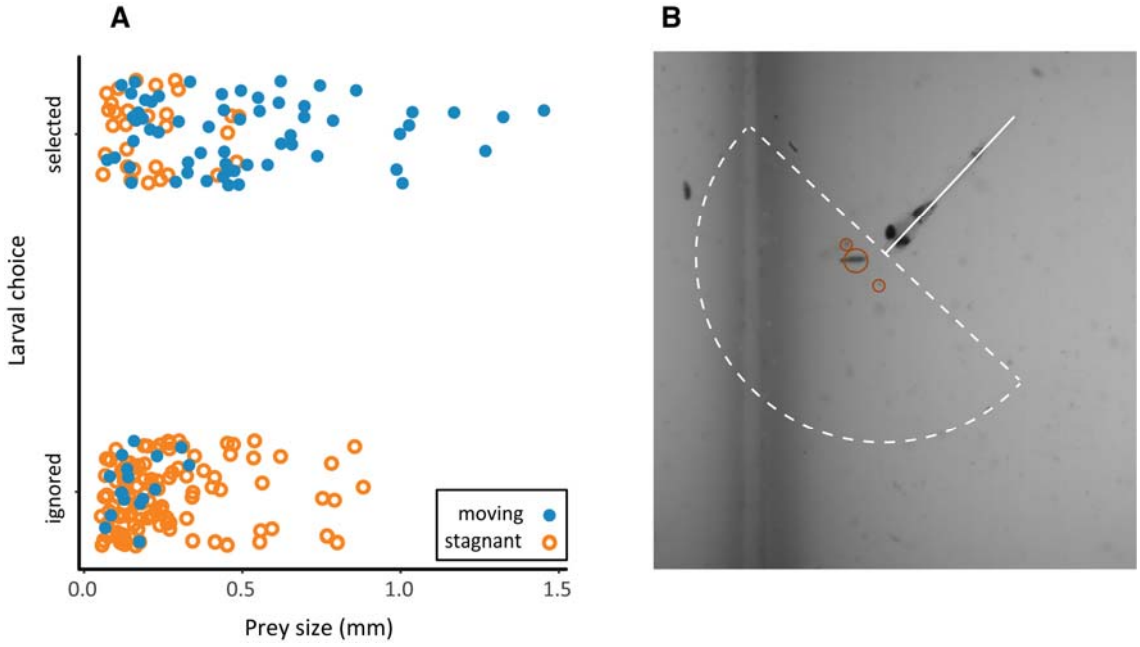

Fig 2. Larvae tended to strike larger, moving prey (Panel A; Table 1). Point colors depict whether the prey was static (orange) or moving (blue) in the 10 frames preceding the strike. Data refer to zooplankton located within an imaginary hemisphere (white dashed line), with a diameter of 1 larval body length, centered at the larvae's mouth (Panel B).

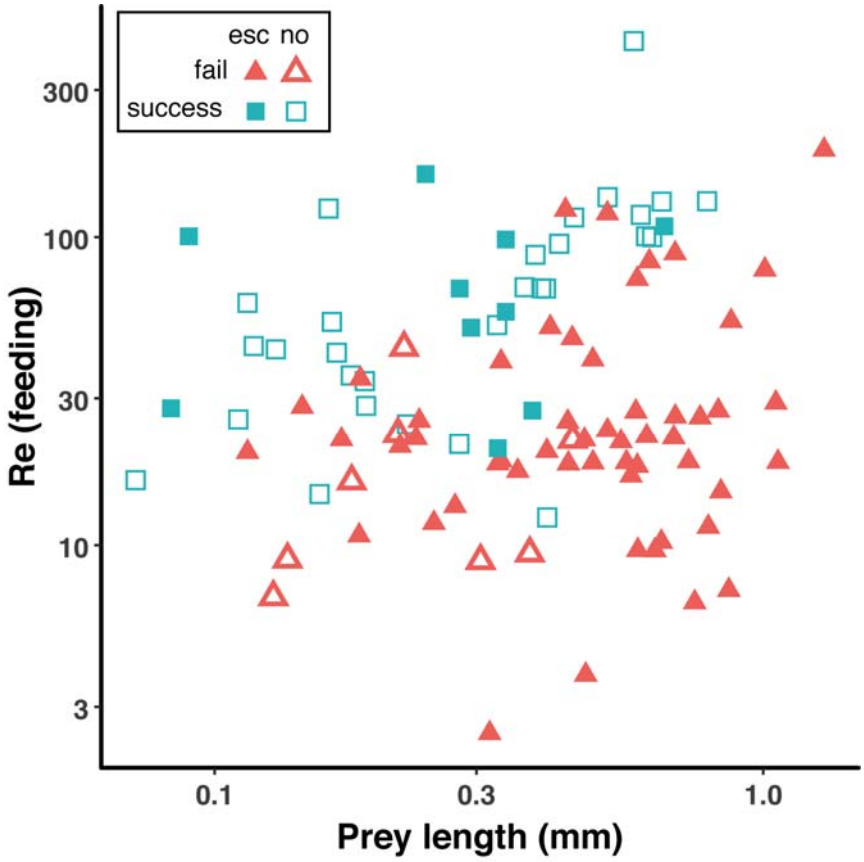

Fig 3. Prey capture success by larval *S. aurata* increased with Re numbers, and decreased for larger prey that elicited an escape response (Table 2). $Re_{(feeding)}$ refers to the Re calculated based on mouth diameter and estimated suction flow speed. Open symbols denote strikes in which the prey did not escape, and full symbols denote strikes in which the prey elicited an escape response. Red triangles indicate larval failure to capture their prey, green squares indicate success. Both X- and Y- axes are plotted on a logarithmic scale.

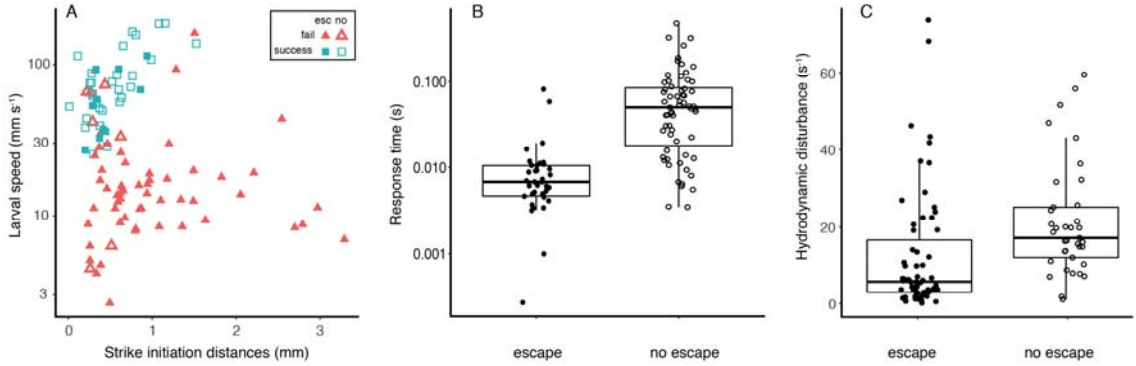

Fig 4. The probability of the prey executing an escape response increased at slower larval swimming speeds and in strikes with longer initiation distances (Panel A; Table 3). Consequently, the response time available for the prey (panel B) was shorter for prey that did not escape (mean ± SE = 0.01 ± 0.0025) than for prey that escaped (mean ± SE = 0.07 ± 0.01). The calculated hydrodynamic disturbance (panel C) was higher for prey that did not escape (mean ± SE = 21.2 ± 2.4 s^{-1}) than for prey that produced an escape response (12.3 ± 2.0 s^{-1}). Open symbols denote strikes in which the prey did not escape, full symbols denote strikes in which the prey produced an escape response. Red triangles in A indicate larval failure to capture their prey, green squares indicate success. Boxes denote the 1st and 3rd quartiles, black horizontal line is the median, and whiskers denote 1.5 inter-quartile range. Note the logarithmic scale for the Y-axis in A and B.